Hidden sector explanation of B-decay and cosmic-ray anomalies

James M. Cline[*]
CERN, Theoretical Physics Department, Geneva, Switzerland
and Department of Physics, McGill University, 3600 Rue University, Montréal, Québec H3A 2T8, Canada

Jonathan M. Cornell[†]
Department of Physics, McGill University, 3600 Rue University, Montréal, Québec H3A 2T8, Canada

David London[‡] and Ryoutaro Watanabe[§]
Physique des Particules, Université de Montréal,
C.P. 6128, succ. centre-ville, Montréal, Québec H3C 3J7, Canada
(Received 16 February 2017; published 19 May 2017)

There are presently several discrepancies in $b \to s\ell^+\ell^-$ decays of B mesons suggesting new physics coupling to b quarks and leptons. We show that a Z', with couplings to quarks and muons that can explain the B-decay anomalies, can also couple to dark matter in a way that is consistent with its relic abundance, direct detection limits, and hints of indirect detection. The latter include possible excess events in antiproton spectra recently observed by the AMS-02 experiment. We present two models, having a heavy (light) Z' with $m_{Z'} \sim 600(12)$ GeV and fermionic dark matter with mass $m_\chi \sim 50(2000)$ GeV, producing excess antiprotons with energies of $\sim 10(300)$ GeV. The first model is also compatible with fits for the Galactic center GeV gamma-ray excess.

DOI: 10.1103/PhysRevD.95.095015

I. INTRODUCTION

At present, there are several measurements of $b \to s\ell^+\ell^-$ decays that suggest the presence of physics beyond the standard model (SM):

(i) The LHCb Collaboration has measured the ratio $R_K \equiv \mathcal{B}(B^+ \to K^+\mu^+\mu^-)/\mathcal{B}(B^+ \to K^+e^+e^-)$, finding $R_K^{\rm expt} = 0.745^{+0.090}_{-0.074}({\rm stat}) \pm 0.036({\rm syst})$ [1]. Thus, a signal of lepton flavor nonuniversality at the level of 25% was found, a deviation of 2.6σ from the SM prediction.

(ii) An angular analysis of $B \to K^*\mu^+\mu^-$ was performed by the LHCb [2,3] and Belle [4] Collaborations, and a discrepancy with the SM in the observable P_5' [5] was found. There are theoretical hadronic uncertainties in the SM prediction, but the deviation can be as large as $\sim 4\sigma$ [6].

(iii) The LHCb Collaboration has measured the branching fraction and performed an angular analysis of $B_s^0 \to \phi\mu^+\mu^-$ [7,8], finding a 3.5σ disagreement with the predictions of the SM, which are based on lattice QCD [9,10] and QCD sum rules [11].

What is particularly intriguing is that all these (independent) discrepancies can be explained if there is new physics (NP) in $b \to s\mu^+\mu^-$. Numerous models have been proposed that generate the correct NP contribution to $b \to s\mu^+\mu^-$ at tree level. They can be put into two categories: those with a Z' vector boson and those containing leptoquarks [12].

Another indication of NP is dark matter (DM); the SM contains no acceptable DM candidate. Moreover the paradigm of WIMP (weakly interacting massive particle) dark matter, which naturally obtains the observed relic density through thermal processes, suggests that the DM mass should be of the order of the electroweak scale. In light of this, it is tempting to ask whether the NP responsible for the B-meson anomalies may be connected to DM. In particular, the new particle that contributes to $b \to s\mu^+\mu^-$ could also be the mediator connecting the DM to SM particles. A simple possibility is that the mediator is a Z' associated with a $U(1)'$, under which the DM is assumed to be charged. We explore this idea here. Previous work in this direction can be found in Refs. [13–16]. Our work has a different emphasis, paying particular attention to recent hints of dark matter annihilation contributing to the antiproton spectrum that has been observed by the AMS-02 experiment [17].

Our starting point is the assumption that, at very high energies, the flavor structure of the SM is gauged [18–21], and the SM group is then extended by the maximal flavor group. It is further assumed that this flavor group is

[*]jcline@physics.mcgill.ca
[†]cornellj@physics.mcgill.ca
[‡]london@lps.umontreal.ca
[§]watanabe@lps.umontreal.ca

spontaneously broken such that the only symmetry left at the scale of $O(\mathrm{TeV})$ is $U(1)'$. Only the left-handed third-generation quarks and second-generation leptons in the flavor basis are charged under this group. [Reference [22] has a similar starting point, but assumes that the unbroken subgroups are $U(1)_q$ in the quark sector and $U(1)_{\mu-\tau}$ in the lepton sector.] The gauge boson associated with $U(1)'$ is denoted by Z'. After electroweak symmetry breaking, when one transforms to the mass basis, a flavor-changing coupling of the Z' to $b_L\bar{s}_L$ is generated, leading to an effective $(\bar{s}_L\gamma^\nu b_L)(\bar{\mu}_L\gamma_\nu\mu_L)$ four-fermion operator. This is used to explain the $b\to s\mu^+\mu^-$ anomalies.

In addition, we assume the presence of a DM fermion χ that is charged under $U(1)'$. When $U(1)'$ is broken, a remnant global $\mathcal{Z}_2$ symmetry remains [23,24], ensuring the stability of χ. The Z' acts as a mediator, enabling the annihilation processes $\chi\bar{\chi}\to Z'\to f\bar{f}$ where f is a SM particle, mainly b_L, t_L, μ_L, ν_μ in our model. For light mediators, the process $\chi\bar{\chi}\to Z'Z'$ can be dominant.

There are two variants of this $U(1)'$ model. In the first, the Z' is heavy, $m_{Z'}=O(\mathrm{TeV})$, the DM χ is a Dirac fermion of mass $m_\chi\sim 30$–70 GeV, and the Z' couples to the χ vectorially. We demonstrate that values of the model parameters can be found such that the NP contribution to $b\to s\mu^+\mu^-$ explains the B anomalies, while remaining consistent with the constraints from $B_s^0-\bar{B}_s^0$ mixing, $b\to s\nu\bar{\nu}$, neutrino trident production, and LHC Z' searches, as well as the DM constraints from relic abundance, and direct and indirect detection. The model also provides a tentative antiproton excess at the 10 GeV energy scale [25,26], as seen in data from AMS-02. An interesting feature of this model is that the invisible contribution to the Z' width from $Z'\to\chi\bar{\chi}$ allows it to escape the stringent LHC limits from dilepton searches ($Z'\to\mu\bar{\mu}$), that would otherwise exclude it.

In addition to the broad antiproton excess found at low (20–100 GeV) energies, there is also tentative evidence for a bumplike feature near the end of the observed AMS-02 $\bar{p}$ spectrum. It has been postulated that this feature could be explained by the production and subsequent acceleration of $\bar{p}$ in supernova remnants [27], but here we consider a dark matter interpretation. Reference [28] showed that the annihilation of multi-TeV DM into highly boosted light mediators, that subsequently decay to quarks, can produce the relatively narrow $\bar{p}$ peak around 300 GeV. We find that a second variant of our model, with $m_{Z'}\cong 12$ GeV and quasi-Dirac DM of mass $m_\chi\cong 1950$ GeV, can give a good fit to this observation, while evading bounds on direct detection due to inelastic couplings of Z' to the DM. This model has strong potential for discovery in upcoming LHC searches.

We begin in Sec. II by defining the model as regards the Z' couplings to SM particles. In Sec. III we derive the space of allowed parameters consistent the various flavor constraints. Section IV augments the model by coupling DM to the Z'. Here we analyze the heavy and light Z' variants of the model in some detail, and demonstrate that it is possible to simultaneously explain the B-decay anomalies and the antiproton excesses. Conclusions are given in Sec. V.

II. MODEL

We start by defining the particle-physics model, at first ignoring its couplings to dark matter, in order to address the anomalies in $b\to s\mu^+\mu^-$. We will later supplement the model (Sec. IV) with couplings to DM.

A. Gauged flavor symmetries

References [18–21] study the effect of gauging the SM (quark or lepton) flavor symmetries. The focus is principally to examine the relation between flavor-violating effects and the Yukawa couplings, especially as regards avoiding too-large flavor-changing neutral currents. An alternative to minimal flavor violation [29,30] is found. A crucial ingredient of the analysis is the addition of new (chiral) fermions to cancel anomalies.

In our model we assume that, at very high energies, the SM gauge group $SU(3)_c\times SU(2)_L\times U(1)_Y$ is extended by the maximal gauged flavor group $SU(3)_Q\times SU(3)_U\times SU(3)_D\times SU(3)_\ell\times SU(3)_E\times O(3)_{\nu_R}$. Here Q (ℓ) corresponds to the left-handed (lh) quarks (leptons), while U, D and E represent the right-handed (rh) up quarks, down quarks and charged leptons, respectively. Three rh neutrinos are included in order to generate neutrino masses via the seesaw mechanism, but are otherwise unimportant for the model. We further assume that the flavor group is spontaneously broken such that the only symmetry left at the TeV scale is $U(1)'$. Only the lh third-generation quarks and second-generation leptons are charged under this group.[1] That is, $SU(3)_U\times SU(3)_D\times SU(3)_E\times O(3)_{\nu_R}$ is broken completely, and $SU(3)_Q\times SU(3)_\ell\to U(1)'$, with associated gauge boson Z'.

B. Yukawa couplings

At the TeV scale the Lagrangian is effective and contains all the terms left from integrating out the heavy fields. Consider the Yukawa terms for the quarks, which connect lh and rh fields. Since only lh third-generation quarks (q_{3L}) are charged under $U(1)'$, any Yukawa term that does not involve q_{3L} is as in the SM: $\lambda_{ij}\bar{q}_{iL}Hq_{jR}+\mathrm{H.c.}$ ($i=1$, 2, $j=1$, 2, 3).

[1]As the underlying flavor group has been made anomaly free by the addition of new fermions, this also resolves all anomaly problems associated with the $U(1)'$. Heavy fermions are required for the anomaly cancellation; we take these to have masses above the scales (TeV) in which we are interested. As a consequence, the only nonstandard fermion that couples to Z' at lower energies is the dark matter.

On the other hand, Yukawa terms that involve q_{3L} are of dimension 5: $[\lambda_j \bar{q}_{3L} H q_{jR} \Phi_q]/M + \mathrm{H.c.}$ $(j = 1,\ 2,\ 3)$, where M is the scale of some integrated-out particles, and Φ is a scalar whose vacuum expectation value breaks $U(1)'$. (For the lepton fields, the Yukawa terms are constructed similarly, except here the lh second-generation leptons are treated like the lh third-generation quarks.) Thus, when Φ gets a vacuum expectation value (VEV), the Lagrangian contains the SM terms, along with the Z' couplings to SM particles, plus higher dimension non-renormalizable terms that can be neglected. At this scale the SM terms include all the Yukawa couplings, $\lambda_{ij} \bar{f}_{iL} H f_{jR} +$ H.c. $(i,\ j = 1,\ 2,\ 3)$.

The simplest UV completion requires the introduction of heavy isosinglet vectorlike quarks T, B, lepton L and scalars Φ_q, Φ_l with U$(1)'$ charges g_q and g_l respectively, that match those of the SM doublets $Q_{3,L}$ and $L_{2,L}$. Then the renormalizable terms

$$\begin{aligned}\mathcal{L} = y'_b \bar{Q}_{3,L} H B_R + y'_t \bar{Q}_{3,L} \tilde{H} T_R + y'_\mu \bar{L}_{2,L} H L_R \\ + \eta_{b,i} \bar{B}_L \Phi_q d_{i,R} + \eta_{t,i} \bar{T}_L \Phi_q u_{i,R} + \eta_{\mu,i} \bar{L}_L \Phi_l e_{i,R} \\ + M_t \bar{T} T + M_b \bar{B} B + M_\mu \bar{L} L \end{aligned} \quad (1)$$

generate the dimension-5 Yukawa interactions after the heavy fermions are integrated out. The corresponding SM Yukawa couplings that are most relevant for this study are

$$\begin{aligned}\lambda_{tt} &= y'_t \eta_{t,t} \frac{\langle \Phi_q \rangle}{M_t} \\ \lambda_{bb} &= y'_b \eta_{b,b} \frac{\langle \Phi_q \rangle}{M_b} \\ \lambda_{bs} &= y'_b \eta_{b,s} \frac{\langle \Phi_q \rangle}{M_b}. \end{aligned} \quad (2)$$

Assuming that $\langle \Phi_q \rangle \sim M_t$, it is possible to generate a large enough top quark Yukawa coupling as long as $y'_t \sim \eta_{t,t} \sim 1$. The quark mixing needed to get the $b \to s$ transitions from Z' exchange will be controlled by $\eta_{b,s}/\eta_{b,b}$.

Since the current limit on vectorlike isosinglet quarks is $M > 870$ GeV [31], the VEV $\langle \Phi_q \rangle$ contributes of order $(870 \times g_q)$ GeV to the Z' mass. We will find that satisfying flavor and dark matter constraints requires $g_q \cong 0.4 m_{Z'}/\mathrm{TeV}$, which is too small for this to be the sole contribution to $m_{Z'}$. The rest must either come from $\langle \Phi_l \rangle$ or from an additional dark scalar field that we will introduce in a scenario with a light Z'. Since the largest Yukawa coupling in the lepton sector that must be generated by $\langle \Phi_l \rangle$ is $\lambda_{\mu\mu}$, we have the freedom to choose $\langle \Phi_l \rangle \ll \langle \Phi_q \rangle$, and we will make this assumption in the light Z' scenario to avoid too large contributions to $m_{Z'}$.

C. Four-fermion operators

In the gauge basis, the Lagrangian describing the couplings of the Z' to fermions is

$$\Delta \mathcal{L}_{Z'} = J^\mu Z'_\mu, \quad (3)$$

$$\text{where } J^\mu = g_q (\bar{\psi}'_q \gamma^\mu P_L \psi'_q) + g_l (\bar{\psi}'_\ell \gamma^\mu P_L \psi'_\ell). \quad (4)$$

Here ψ'_q (ψ'_ℓ) represents both t and b (ν_μ and μ^-) fields, and the primes indicate the gauge basis. $g_q = g_1 Q_q$ and $g_l = g_1 Q_\ell$ are the couplings of the Z' to quarks and leptons, respectively [g_1 is the $U(1)'$ coupling constant, and Q_q and Q_ℓ are the $U(1)'$ charges of quarks and leptons]. Once the heavy Z' is integrated out, we obtain the following effective Lagrangian containing 4-fermion operators:

$$\begin{aligned}\mathcal{L}^{\mathrm{eff}}_{Z'} &= -\frac{1}{2 m_{Z'}^2} J_\mu J^\mu \\ &\supset -\frac{g_q g_l}{m_{Z'}^2} (\bar{\psi}'_q \gamma_\mu P_L \psi'_q)(\bar{\psi}'_\ell \gamma^\mu P_L \psi'_\ell) \\ &\quad - \frac{g_q^2}{2 m_{Z'}^2} (\bar{\psi}'_q \gamma_\mu P_L \psi'_q)(\bar{\psi}'_q \gamma^\mu P_L \psi'_q) \\ &\quad - \frac{g_l^2}{2 m_{Z'}^2} (\bar{\psi}'_\ell \gamma_\mu P_L \psi'_\ell)(\bar{\psi}'_\ell \gamma^\mu P_L \psi'_\ell). \end{aligned} \quad (5)$$

The first 4-fermion operator (two quarks and two leptons) is relevant for $b \to s \ell^+ \ell^-$ and $b \to s \nu \bar{\nu}$ decays, the second operator (four quarks) contributes to processes such as $B_s^0 - \bar{B}_s^0$ mixing, and the third operator (four leptons) contributes to neutrino trident production and $Z \to 4\mu$.

In order to obtain the operators involving the physical fields, we must transform the fermions to the mass basis. We make the approximation that the gauge and mass eigenstates are the same for all fermions except the lh up- and down-type quarks. In the lepton sector, this holds if neutrino masses are neglected. For the quarks, it would be a good approximation if λ_{sb}, which comes from the usual dimension-4 Yukawa interaction, happens to be much smaller than λ_{bs} in Eq. (2). In this case the mixing angle between second and third generation left-handed quarks is approximately $\theta_L \cong \eta_{b,s}/\eta_{b,b}$ while that of their right-handed counterparts is smaller by a factor of $\sim m_s/m_b$. In the following we therefore ignore θ_R.

In transforming from the gauge basis to the mass basis, we then have

$$u'_L = U u_L, \qquad d'_L = D d_L, \quad (6)$$

where U and D are 3×3 unitary matrices and the spinors $u^{(\prime)}$ and $d^{(\prime)}$ include all three generations of fermions. The CKM matrix is given by $V_{\mathrm{CKM}} = U^\dagger D$.

For the B anomalies, we are particularly interested in the decay $b \to s \mu^+ \mu^-$, i.e., the Z' must couple to $\bar{s} b$ in the mass basis. If the Z' also couples to $\bar{d}s$ ($\bar{d}b$), there are stringent constraints from $K^0-\bar{K}^0$ ($B^0-\bar{B}^0$) mixing. To avoid this, we assume that the D transformation involves only the second and third generations [32,33]

$$D = \begin{pmatrix} 1 & 0 & 0 \\ 0 & \cos\theta_D & \sin\theta_D \\ 0 & -\sin\theta_D & \cos\theta_D \end{pmatrix}, \tag{7}$$

where $\theta_D = \theta_L \cong \eta_{b,s}/\eta_{b,b}$ as mentioned above. With this transformation, for the down-type quarks, couplings involving the second generation (possibly flavor-changing) are generated in the mass basis. (For the up-type quarks, the first generation can also be involved.)

Now, we are interested in $b \to s$ transitions in the mass basis, and these can arise through the exchange of a Z'. Applying the above transformation to Eq. (5), we find the following. The 4-fermion operator applicable to $b \to s\mu^+\mu^-$ or $b \to s\nu\bar{\nu}$ is

$$\frac{g_q g_l}{m_{Z'}^2} \sin\theta_D \cos\theta_D (\bar{s}\gamma_\mu P_L b)(\bar{L}\gamma^\mu P_L L). \tag{8}$$

For $B_s^0-\bar{B}_s^0$ mixing, the relevant operator is

$$-\frac{g_q^2}{2m_{Z'}^2} \sin^2\theta_D \cos^2\theta_D (\bar{s}\gamma^\mu P_L b)(\bar{s}\gamma^\mu P_L b). \tag{9}$$

D. $Z'd\bar{d}$ and $Z'u\bar{u}$ couplings

Although our immediate concern is $b \to s$ transitions, the small couplings of Z' to light quarks induced by mixing in our model will be relevant later on, for the direct detection of dark matter. Because the D transformation involves only the second and third generations [Eq. (7)], the $Z'd\bar{d}$ coupling vanishes. Using $V_{\rm CKM} = U^\dagger D$, the Z' coupling to lh up-type quarks is given by

$$M = U^\dagger \begin{pmatrix} 0 & 0 & 0 \\ 0 & 0 & 0 \\ 0 & 0 & 1 \end{pmatrix} U = V_{\rm CKM} D^\dagger \begin{pmatrix} 0 & 0 & 0 \\ 0 & 0 & 0 \\ 0 & 0 & 1 \end{pmatrix} D V_{\rm CKM}^\dagger. \tag{10}$$

The $Z'u\bar{u}$ coupling is then given by

$$M_{11} = |V_{us}|^2 \sin^2\theta_D - 2{\rm Re}(V_{us}V_{ub}^*) \sin\theta_D \cos\theta_D + |V_{ub}|^2 \cos^2\theta_D. \tag{11}$$

For very small θ_D such that $\sin\theta_D \cong \theta_D$ and $\cos\theta_D \cong 1$, and neglecting the phase in $V_{us}V_{ub}^*$, we can estimate $M_{11} \sim |V_{ub} - \theta_D V_{us}|^2$.

III. FLAVOR CONSTRAINTS

Here we determine the allowed values of θ_D versus $g_q g_l/m_{Z'}^2$ that can explain the $b \to s\mu^+\mu^-$ anomalies, while respecting constraints from $B_s^0-\bar{B}_s^0$ mixing, $b \to s\nu\bar{\nu}$, neutrino trident production, $Z \to 4\mu$ decays, and the muon anomalous magnetic moment.

A. $b \to s\mu^+\mu^-$

$b \to s\mu^+\mu^-$ transitions are described by the effective Hamiltonian

$$H_{\rm eff} = -\frac{\alpha G_F}{\sqrt{2}\pi} V_{tb} V_{ts}^* \sum_{a=9,10} (C_a O_a + C'_a O'_a),$$
$$O_{9(10)} = [\bar{s}\gamma_\mu P_L b][\bar{\mu}\gamma^\mu(\gamma_5)\mu], \tag{12}$$

where the primed operators are obtained by replacing L with R. The Wilson coefficients $C_a^{(\prime)}$ include both SM and NP contributions. In Ref. [6], a global analysis of the $b \to s\ell^+\ell^-$ anomalies was performed for both electron and muon decay modes, including data on $B \to K^{(*)}\mu^+\mu^-$, $B \to K^{(*)}e^+e^-$, $B_s^0 \to \phi\mu^+\mu^-$, $B \to X_s\mu^+\mu^-$, $b \to s\gamma$ and $B_s^0 \to \mu^+\mu^-$. Theoretical hadronic uncertainties were taken into account, and it was found that there is a significant disagreement with the SM, possibly as large as 4σ. This discrepancy can be explained if there is NP in $b \to s\mu^+\mu^-$. There are four possible explanations, each having roughly equal goodness-of-fits, but the one that interests us is $C_9^{\rm NP} = -C_{10}^{\rm NP} < 0$. According to the fit, the allowed 3σ range for the Wilson coefficients is

$$-1.12 \le C_9^{\rm NP} = -C_{10}^{\rm NP} \le -0.18. \tag{13}$$

In our model, $b \to s\mu^+\mu^-$ transitions are given by the effective Hamiltonian

$$H_{\rm eff}(b \to s\mu^+\mu^-) = \left(-\frac{\alpha G_F}{\sqrt{2}\pi} V_{tb} V_{ts}^* C_9^{\rm SM} + \frac{g_q g_l}{2m_{Z'}^2} \sin\theta_D \cos\theta_D\right) \times (\bar{s}\gamma^\mu P_L b)(\bar{\ell}_i \gamma_\mu (1-\gamma^5)\ell_j), \tag{14}$$

where the SM contribution, $C_9^{\rm SM}(= -C_{10}^{\rm SM}) \simeq 0.94$ [34], encodes a loop suppression. This leads to

$$C_9^{\rm NP} = -C_{10}^{\rm NP} = \frac{\pi}{\sqrt{2}\alpha G_F V_{tb} V_{ts}^*} \frac{g_q g_l}{m_{Z'}^2} \sin\theta_D \cos\theta_D \tag{15}$$

in $b \to s\mu^+\mu^-$, while there is no NP contribution to $b \to se^+e^-$. Equation (13) then constrains the combination of theoretical parameters $\theta_D g_q g_l/m_{Z'}^2$ in the limit of small θ_D.

B. $B_s^0 - \bar{B}_s^0$ mixing

In our model, $B_s^0 - \bar{B}_s^0$ mixing is described by the effective Hamiltonian

$$H_{\rm eff} = \left(N C_{VLL}^{\rm SM} + \frac{g_q^2}{2m_{Z'}^2} \sin^2\theta_D \cos^2\theta_D \right) \times (\bar{s}\gamma^\mu P_L b)(\bar{s}\gamma_\mu P_L b), \quad (16)$$

where $N = (G_F^2 m_W^2/16\pi^2)(V_{tb}V_{ts}^*)^2$ (the SM contribution is produced via a box diagram), and $C_{VLL}^{\rm SM} \simeq 4.95$ [33]. The mass difference in the B_s system is then given by

$$\Delta M_s = \frac{2}{3} m_{B_s} f_{B_s}^2 \hat{B}_{B_s} \times \left| N C_{VLL}^{\rm SM} + \frac{g_q^2}{2m_{Z'}^2} \sin^2\theta_D \cos^2\theta_D \right|. \quad (17)$$

The SM prediction is [33]

$$\Delta M_s^{\rm SM} = (17.4 \pm 2.6)\ {\rm ps}^{-1}. \quad (18)$$

This is to be compared with the experimental measurement [35]

$$\Delta M_s = (17.757 \pm 0.021)\ {\rm ps}^{-1}, \quad (19)$$

leading to a constraint on $\theta_D^2 g_q^2/m_{Z'}^2$ for $\theta_D \ll 1$.

In the SM, the weak phase of $B_s^0 - \bar{B}_s^0$ mixing is predicted to be very small: $\varphi_s = -0.03704 \pm 0.00064$ [36,37]. The present measurement of this quantity is $\varphi_s^{c\bar{c}s} = -0.030 \pm 0.033$ [35]. Although these values are consistent with one another, the experimental error is large, allowing for a significant NP contribution. This then raises the question: could the present Z' model give a large contribution to φ_s? Unfortunately, the answer is no. The Z' contribution to $B_s^0 - \bar{B}_s^0$ mixing is given in Eq. (17). It can include a weak phase only if g_q is complex. However, from Eq. (3), we see that, since the coupling is self conjugate, the coupling constant g_q is real. Thus, if a future measurement of $\varphi_s^{c\bar{c}s}$ were to find a sizeable deviation from the SM, it could not be accommodated in our model.

C. $b \to s\nu\bar{\nu}$

In our model, the effective Hamiltonian for $b \to s\nu\bar{\nu}$ is

$$H_{\rm eff}(b \to s\nu_\mu\bar{\nu}_\mu) = \left(-\frac{\alpha G_F}{\sqrt{2}\pi} V_{tb}V_{ts}^* C_L^{\rm SM} + \frac{g_q g_l}{2m_{Z'}^2} \sin\theta_D \cos\theta_D \right) \times (\bar{s}\gamma^\mu P_L b)(\bar{\nu}_\mu\gamma_\mu(1-\gamma^5)\nu_\mu), \quad (20)$$

where the SM loop function is $C_L^{\rm SM} \simeq -6.60$. The NP contribution can be constrained by the 90% C.L. upper limits of $\mathcal{B}(B^+ \to K^+\nu\bar{\nu}) \le 1.7 \times 10^{-5}$, $\mathcal{B}(B^+ \to K^{*+}\nu\bar{\nu}) \le 4.0 \times 10^{-5}$, and $\mathcal{B}(B^0 \to K^{*0}\nu\bar{\nu}) \le 5.5 \times 10^{-5}$, given by the *BABAR* and Belle Collaborations [38,39].

Comparing the experimental upper limits with the SM predictions, the resulting constraint (including theoretical uncertainties) is [40]

$$\frac{2|C_L^{\rm SM}|^2 + |C_L^{\rm SM} + C_L^{\rm NP}|^2}{3|C_L^{\rm SM}|^2} \lesssim 5, \quad (21)$$

with

$$C_L^{\rm NP} = \frac{\pi}{\sqrt{2}\alpha G_F V_{tb}V_{ts}^*} \frac{g_q g_l}{m_{Z'}^2} \sin\theta_D \cos\theta_D. \quad (22)$$

This has the same form as the NP contribution to $b \to s\mu^+\mu^-$ [Eq. (15)]. However, as we will see below, the constraint from $b \to s\nu\bar{\nu}$ is quite a bit weaker than that from $b \to s\mu^+\mu^-$.

D. Neutrino trident production

A further constraint arises due to the effect of the Z' boson on the production of $\mu^+\mu^-$ pairs in neutrino-nucleus scattering, $\nu_\mu N \to \nu_\mu N \mu^+\mu^-$ (neutrino trident production). At leading order, this process is effectively $\nu_\mu\gamma \to \nu_\mu\mu^+\mu^-$, which in the SM is produced by single-W/Z exchange diagrams. With respect to the effective Lagrangian, it corresponds to the four-fermion effective operator

$$\mathcal{L}_{\rm eff:trident} = [\bar{\mu}\gamma^\mu(C_V - C_A\gamma^5)\mu][\bar{\nu}\gamma_\mu(1-\gamma^5)\nu], \quad (23)$$

with an external photon coupling to μ^+ or μ^-. In the SM, we have $C_V^{\rm SM} \ne C_A^{\rm SM}$ in Eq. (23). Combining both W- and Z-exchange diagrams, we have [41–44]

$$C_V^{\rm SM} = -\frac{g^2}{8m_W^2}\left(\frac{1}{2} + 2\sin^2\theta_W\right), \quad C_A^{\rm SM} = -\frac{g^2}{8m_W^2}\frac{1}{2}. \quad (24)$$

On the other hand, the Z' boson contributes to Eq. (23) with the pure $V - A$ form,

$$C_V^{\rm NP} = C_A^{\rm NP} = -\frac{g_l^2}{4m_{Z'}^2}. \quad (25)$$

In terms of the coefficients C_V and C_A, the inclusive cross section is given by,[2] [45]

[2]The interference term $C_V C_A$ is omitted in Eq. (26). According to the study in Ref. [44], this term is suppressed by an order of magnitude compared to the $(C_{V,A})^2$ terms.

$$\sigma(\hat{s}) \simeq (C_V^2 + C_A^2)\frac{2\alpha_{\rm EM}\hat{s}}{9\pi^2}\left[\log\left(\frac{\hat{s}}{m_\mu^2}\right) - \frac{19}{6}\right], \quad (26)$$

for $\hat{s} = (p_\nu + p_\gamma)^2$, where p_ν and p_γ are the initial momenta of the neutrino and photon, respectively. The existing experimental result [46] for $\sigma(\nu N \to \nu N \mu^+\mu^-)$ is compared with $\int \sigma(\hat{s})P(\hat{s}, q^2)$, where $P(\hat{s}, q^2)$ is the probability of creating a virtual photon in the Coulomb field of the nucleus (for example, see Ref. [45]). Alternatively, we can compare the ratio of the experimental data and the SM prediction reported as [16,45]

$$\left.\frac{\sigma_{\rm exp}}{\sigma_{\rm SM}}\right|_{\nu N\to\nu N\mu^+\mu^-} = 0.82 \pm 0.28, \quad (27)$$

with the theoretical prediction

$$\left.\frac{\sigma_{\rm SM+NP}}{\sigma_{\rm SM}}\right|_{\nu N\to\nu N\mu^+\mu^-} \simeq \frac{\sigma_{\rm SM+NP}(\hat{s})}{\sigma_{\rm SM}(\hat{s})} = \frac{(C_V^{\rm SM} + C_V^{\rm NP})^2 + (C_A^{\rm SM} + C_A^{\rm NP})^2}{(C_V^{\rm SM})^2 + (C_A^{\rm SM})^2}. \quad (28)$$

The net effect is that this will provide an upper limit on $g_l^2/m_{Z'}^2$.

E. $Z \to 4\mu$

A constraint similar to that from neutrino trident production comes from the process $Z \to \mu\mu^*$, $\mu^* \to \mu Z'^*$, $Z'^* \to \mu\mu$, resulting in $Z \to 4\mu$. The decay mode into light leptons (e, μ) has been measured by ATLAS and CMS, giving a branching ratio consistent with the SM value, 3.3×10^{-6} [47]. The NP contribution is suppressed for heavy Z', $m_{Z'} > m_Z$, giving a weak constraint, but is larger when $m_{Z'} < m_Z$ so that the intermediate Z' can be on shell. In this case we can estimate the NP contribution (ignoring interference with the SM) as

$$\Gamma(Z \to 4\mu) = \Gamma(Z \to Z'\mu^+\mu^-)B(Z' \to \mu^+\mu^-). \quad (29)$$

In our later fit to the AMS-02 antiproton excess, we will be interested in $m_{Z'} \cong 12$ GeV. The predicted branching ratio (evaluated with the use of MADGRAPH 5 [48,49]) is shown in Fig. 1 for this case, giving the constraint $g_l < 0.05$. The result depends upon g_q since this affects the branching ratio of $Z' \to \mu^+\mu^-$,

$$B(Z' \to \mu^+\mu^-) = \frac{g_l^2}{2g_l^2 + 1.9g_q^2}, \quad (30)$$

taking account of the phase-space and amplitude suppression for decays into $b\bar{b}$. For definiteness we have taken $g_q = g_l$; larger values of g_q will weaken the constraint on g_l. Our result is consistent with the limits obtained in Refs. [45,50].

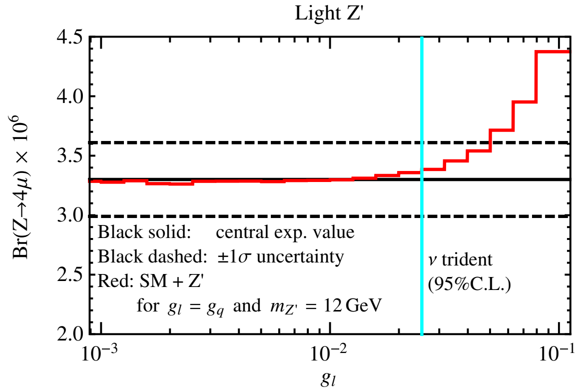

FIG. 1. Solid (red): predicted branching ratio for $Z \to 4\mu$ via $Z \to Z'\mu^+\mu^-$ for light Z', $m_{Z'} = 12$ GeV, versus g_l. Horizontal lines denote the 1σ experimentally allowed region. Vertical line is upper limit from ν trident production.

The constraint from $Z \to 4\mu$ is relatively weak; in the case $g_q = g_l$, the maximum value of g_l consistent with neutrino trident production (see Fig. 2) is $g_l \cong 2m_{Z'}/\text{TeV} \cong 0.02$, which is more stringent than that from $Z \to 4\mu$.

F. Muon $g - 2$

There has been a long-standing 3.6σ discrepancy between the predicted and measured values of the anomalous magnetic moment of the muon, a_μ. To address this,

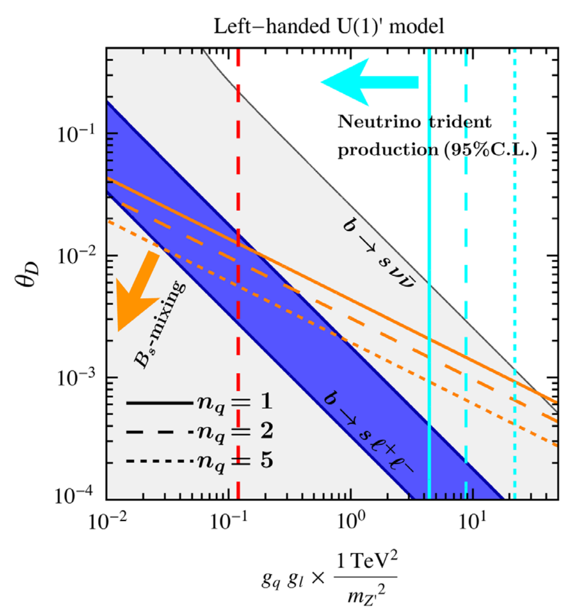

FIG. 2. Allowed regions from flavor constraints, for several values of $n_q \equiv g_q/g_l$; dark (blue) band gives observed R_K. The preferred couplings from dark matter constraints (for the heavy Z' model) are shown by the vertical red dashed line (from the $n_q = 2$, $n_\chi = 5$ model, where $n_q = g_q/g_l$ and $n_\chi = g_\chi/g_q$).

TABLE I. Summary of the flavor constraints from $b \to s\mu^+\mu^-$, $b \to s\nu\bar{\nu}$, $B_s^0 - \bar{B}_s^0$ mixing, and $\nu N \to \nu N \mu^+\mu^-$, where $\hat{m}_{\rm TeV} \equiv m_{Z'}/1$ TeV and $s_\theta c_\theta = \sin\theta_D \cos\theta_D$.

Process	Constraint	Range
$b \to s\mu^+\mu^-$	$0.00028 \le g_q g_l s_\theta c_\theta \hat{m}_{\rm TeV}^{-2} \le 0.00177$	"3σ" [6]
$b \to s\nu\bar{\nu}$	$\lvert 0.01041 + g_q g_l s_\theta c_\theta \hat{m}_{\rm TeV}^{-2} \rvert \lesssim 0.03711$	90% C.L.
$B_s^0 - \bar{B}_s^0$ mixing	$g_q^2 (s_\theta c_\theta)^2 \hat{m}_{\rm TeV}^{-2} \lesssim 0.00002$	(1σ theoretical error)
$\nu N \to \nu N \mu^+\mu^-$	$g_l^2 \hat{m}_{\rm TeV}^{-2}(1 + 0.02097 \times g_l^2 \hat{m}_{\rm TeV}^{-2}) \le 4.81193$	95% C.L.

models have been proposed that include a Z' with off diagonal vectorial couplings to μ and a heavier lepton (ℓ). (The case where ℓ is a new lepton L is discussed in Ref. [51]; $\ell = \tau$ is examined in Ref. [52].) This leads to a $(m_\ell/m_{Z'})^2$ enhancement of the loop contribution to a_μ.

In the present model, the Z' couples only to μ (and has $V - A$ couplings). The contribution to a_μ now increases the discrepancy, though its actual size is too small to be relevant. For example, in our model with $m_{Z'} = 12$ GeV, the contribution to a_μ is negligible as long as $g_l \lesssim 0.02$. And it does not help to allow the Z' to couple to both μ and τ (with off diagonal $\mu - \tau$ couplings). In this case, there is then a tree-level Z' contribution to $\tau \to 3\mu$, which is strongly constrained.

G. Allowed parameter space

The preceding flavor constraints are summarized in Table I, where $V_{tb}V_{ts}^* = -0.0405 \pm 0.0012$ [47] and $f_{B_s}\hat{B}_{B_s}^{1/2} = (266 \pm 18)$ MeV [53] have been used, and where $\hat{m}_{\rm TeV} \equiv m_{Z'}/1$ TeV. Concerning $B_s^0 - \bar{B}_s^0$ mixing, the experimental value is precisely determined (of order 0.1%) while the theory prediction has a large uncertainty. We take a 1σ range for the theoretical uncertainty to obtain the constraint.

In Fig. 2, we combine all the constraints to determine the space of allowed values of the theoretical parameters in the $(g_q g_l \hat{m}_{\rm TeV}^{-2}, \theta_D)$ plane, for several values of $n_q \equiv g_q/g_l$. The area in the dark (blue) region below the B_s mixing lines (orange) and to the left of the neutrino trident lines (cyan) can explain the $b \to s\mu^+\mu^-$ anomalies, consistent with all the other constraints.

Note that Fig. 2 applies for $m_{Z'} \gg m_b$. However, for the light-Z' scenario ($m_{Z'} = 12$ GeV), the parameter $g_q g_l/m_{Z'}^2$ should be (approximately) replaced by $g_q g_l/(m_{Z'}^2 - m_b^2)$.

IV. DARK MATTER MODELS

There are two independent tentative anomalies in the AMS-02 antiproton spectrum: one at low ~10 GeV energies and one at ~300 GeV. To alternatively address them, we consider two possible extensions of the model to include dark matter: (1) TeV-scale Z', and Dirac dark matter of mass 30–70 GeV, and (2) 10 GeV-scale Z', coupled to two quasidegenerate Majorana DM states with masses $m_\chi \sim 2$ TeV. In the second model, the Z' couples off diagonally to the DM mass eigenstates, alleviating direct detection signals. A consistent treatment of the second model requires the inclusion of the dark Higgs boson that gives mass to the Z'.

A. Heavy Z', Dirac dark matter

We first consider the scenario in which the DM χ is a Dirac particle with mass $m_\chi \ll m_{Z'}$ and vectorial coupling to the Z' with strength g_χ. In the approximation of small mixing angles, where we neglect the couplings to lower-generation quarks, the Z' can be integrated out to give the effective Hamiltonian

$$H = \frac{g_q g_\chi}{m_{Z'}^2} \sum_{i=t,b} (\bar{q}_i \gamma_\mu P_L q_i)(\bar{\chi}\gamma^\mu \chi) + \frac{g_l g_\chi}{m_{Z'}^2} \sum_{j=\mu,\nu_\mu} (\bar{l}_j \gamma_\mu P_L l_j)(\bar{\chi}\gamma^\mu \chi). \tag{31}$$

As in the preceding sections, we assume that the Z' couples only to left-handed SM particles.

1. Astrophysical constraints

The cross section for $\chi\bar{\chi}$ annihilation into b_L quarks and μ_L, ν_μ leptons is given by

$$\langle \sigma v \rangle = \frac{(3g_q^2 + 2g_l^2) m_\chi^2}{2\pi} \left(\frac{g_\chi}{m_{Z'}^2}\right)^2 \cong 4.4 \times 10^{-26} \ \frac{\rm cm^3}{\rm s} \tag{32}$$

to get the right relic density [54]. This is the appropriate formula for $m_\chi < m_t$, as suggested by the best-fit regions for AMS excess antiprotons, $m_\chi \in [30\text{–}70]$ GeV [26], or $m_\chi \cong 80$ GeV [25].[3]

To get a large enough antiproton signal, consistent with the thermal relic annihilation cross section, we want quarks

[3]Reference [55] finds a larger DM mass of $m_\chi \cong 200$ GeV as the best-fit point, which would give a larger predicted cross section, with $(3g_q^2 + 3g_l^2) \to (10.1 g_q^2 + 3g_l^2)$, due to the production of top quark pairs with some phase-space suppression $[(1 - m_t^2/m_\chi^2)^{1/2}]$, compensated by matrix element enhancement $(1 + m_t^2/2m_\chi^2)$. We find this scenario is difficult to reconcile with the global constraints, and hence do not further consider it.

to dominate in the final state. Reducing the relative coupling to leptons also helps to alleviate stringent LHC constraints considered below, but at the same time diminishes the NP contribution to $b \to s\mu^+\mu^-$. We find that taking $g_q = n_q g_l$ with $n_q = 2$ is a sufficient compromise, implying that annihilation into b quarks makes up 86% of the total cross section. This leaves just one ratio $g_\chi/g_q \equiv n_\chi$ to be constrained. We then have from Eq. (32)

$$g_\chi = \frac{1.09\sqrt{n_\chi}}{\hat{m}_{70}^{1/2}} \frac{m_{Z'}}{\text{TeV}},$$
$$g_q = 2g_l = \frac{1.09}{\sqrt{n_\chi}\hat{m}_{70}^{1/2}} \frac{m_{Z'}}{\text{TeV}}, \tag{33}$$

where $\hat{m}_{70} \equiv m_\chi/(70\ \text{GeV})$.

The couplings in (33) are evaluated at the scale of m_χ, after integrating out the heavy Z' at the scale of its mass. It has been pointed out in Ref. [56] that running of the $\text{U}(1)'$ coupling in dark matter models can sometimes be important. However below the Z' threshold, no significant running is expected because the Z' is heavy and has already been removed from the effective theory. We have estimated this effect by computing the vertex correction with loop momenta between m_χ and $m_{Z'}$ with a massive Z' propagator, finding that $\Delta g_\chi \sim 3 \times 10^{-3} g_\chi^3$. On the other hand, above $m_{Z'}$ running can become significant, and one can wonder whether perturbation theory may break down at scales not far above $m_{Z'}$.

To estimate whether this is the case in the present model, we integrate the beta function $dg_\chi/d\ln\mu = g_\chi^3/12\pi^2$ between $m_{Z'}$ and a UV scale Λ, finding that $\alpha_\chi = g_\chi^2/4\pi \gtrsim 1$ already at $\Lambda = 10$ TeV for $m_{Z'} = 1.2$ TeV, while for smaller $m_{Z'}$ the scale of nonperturbativity quickly rises to much higher values, as shown in Fig. 3. Therefore lighter $m_{Z'} \lesssim 1$ TeV are preferred for consistency of the theory up to scales above ~100 TeV, where some UV completion could be expected.

The most recent Fermi-LAT searches for emission from dark matter annihilation in dwarf spheroidal galaxies currently exclude cross sections of $\langle\sigma v\rangle > 1.9 \times 10^{-26}\ \text{cm}^3/\text{s}$ at 95% C.L. for 80 GeV DM annihilating to $b\bar{b}$ [57]. This is in tension with the cross sections suggested by the DM interpretation of the $\bar{p}$ excess. However, recent works [58,59] have pointed out that the dark matter content of some of the dwarf spheroidals in the Fermi analysis may have been overestimated, resulting in a less stringent limit that can be compatible with DM explanations of cosmic ray excesses.

2. Collider limits

ATLAS and CMS have searched for resonant lepton pairs from $Z' \to \ell\bar{\ell}$ [60,61]. These depend on the branching ratio of Z' into $\mu^+\mu^-$, which in our model is given by

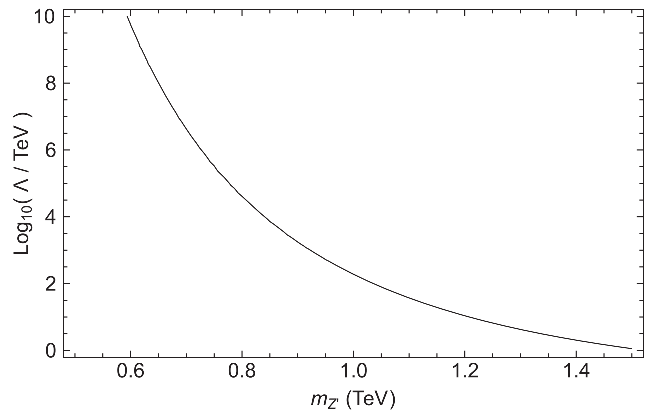

FIG. 3. The UV scale Λ where $\alpha_\chi = g_\chi^2/4\pi = 1$, versus $m_{Z'}$, using the relic density value of g_χ from (33) at the scale $m_\chi = 70$ GeV as the IR boundary condition for renormalization group (RG) running.

$$B(\mu\bar{\mu}) = \frac{g_l^2}{3(1+f)g_q^2 + 2g_l^2 + 2g_\chi^2}$$
$$= \frac{0.25}{3.5 + 3f + 2n_\chi^2}, \tag{34}$$

where $f = (1 + 7x/17)\sqrt{1 - 4x^2}$ with $x = (m_t/m_{Z'})^2$ for top quark final states [62]. It is common in model-building to forbid Z' couplings to leptons in order to avoid these stringent dilepton constraints. Here we manage to satisfy them by coupling the Z' only to the b-quarks present in the proton, leading to PDF suppression of the production cross section, combined with a reduction in the partial width of Z' to leptons due to the invisible decays $Z' \to \chi\bar{\chi}$.

We show the ATLAS dilepton limit in Fig. 4 (left), along with predictions for the model with $g_l = g_q/n_q = 0.5g_q$, $g_\chi = n_\chi g_q = 5g_q$, and $m_\chi = 70$ GeV, for which the region with 300 GeV $< m_{Z'} <$ 390 GeV is excluded. These were calculated by computing the production cross section for Z' through its coupling to b-quarks using MADGRAPH 5 [48,49], with a QCD K-factor correction that happens to be unity within uncertainties of ~10%–30% (see Fig. 3 of Ref. [63]). Then Eq. (33) implies $g_l g_q/m_{Z'}^2 = 0.12/\text{TeV}^2$, which is shown as the vertical line in the parameter space relevant for $b \to s\mu^+\mu^-$, Fig. 2. The blue region below the dashed lines, showing the upper bound on the quark mixing angle from B_s mixing, is allowed.

Equation (33) demands a large coupling g_χ unless $m_{Z'}$ is in the lower part of its allowed region. For example, with $m_{Z'} = 250$ GeV, we obtain $g_\chi = 0.6$ (and it scales linearly with $m_{Z'}$ for larger values). Taking larger values of m_χ reduces the couplings needed to get the right relic density, and further alleviates tension with the dilepton search, but it also pushes $g_q g_l/m_{Z'}^2$ further to the left in Fig. 2, making it difficult to get a large enough contribution to $b \to s\mu^+\mu^-$. This is the problem with the scenario with $m_\chi = 200$ GeV (see footnote 3).

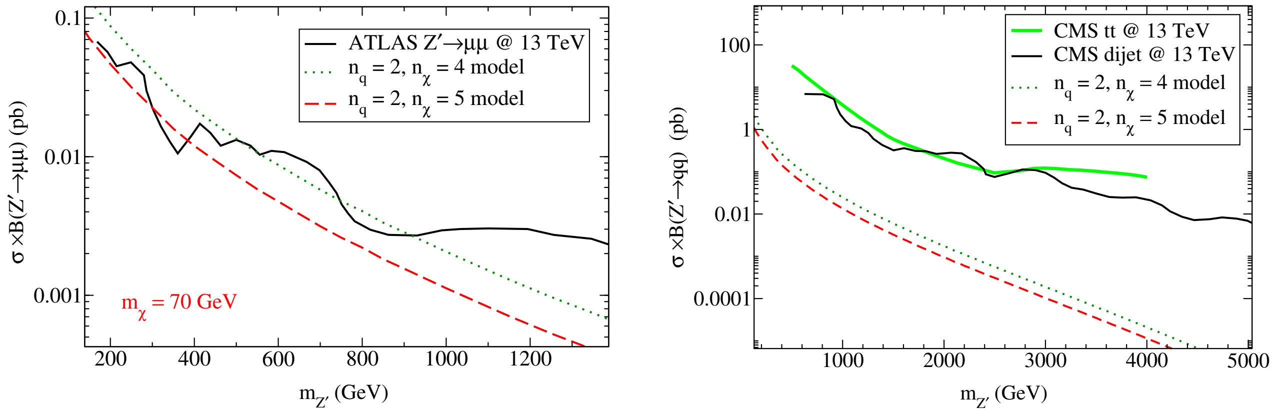

FIG. 4. Left: ATLAS limit on $pp \to Z' \to \mu\bar{\mu}$ production and decay, and predictions of two models that are close to the constraint; right: same for $pp \to Z' \to b\bar{b}$ or $t\bar{t}$ as limited by searches for dijet or $t\bar{t}$ final states. The dijet limit is adjusted upward from the published value of $\sigma B_{qq} A$ by assuming the event acceptance is $A = 0.6$ [64].

There are also limits from resonant dijet searches from $b\bar{b}$ or $t\bar{t}$ final states [64–67] but which are weaker than those from the dilepton searches. The branching ratio to b quarks is 12 times greater than Eq. (34), but the predicted cross section is still far below the limit, as shown in Fig. 4 (right).

3. Direct detection

The couplings of Z' to light quarks in this model are highly suppressed, making the tree-level contribution to χ-nucleon scattering well below the current limit. The coupling of Z' to left-handed up quarks due to mixing is of order [see Eq. (11)]

$$g_u \sim |\theta_D V_{us} - V_{ub}|^2 g_q \sim 6 \times 10^{-6} g_q \qquad (35)$$

for the maximal quark mixing angle $\theta_D = 0.008$ indicated in Fig. 2. The effective cross section on nucleons is given by[4] [68]

$$\sigma_N = \frac{(g_\chi g_u m_n)^2}{4\pi m_{Z'}^4}(1 + Z/A)^2 \cong 2 \times 10^{-51}\ \text{cm}^2, \qquad (36)$$

using Eqs. (33) and (35) with $m_\chi = 70$ GeV, where m_n is the nucleon mass. This is well below the expected reach of the LZ experiment, 2×10^{-48} cm^2 [69].

However, the coupling of Z' to quarks and leptons contributes at one loop to kinetic mixing, $(\epsilon/2) F^{\mu\nu} Z'_{\mu\nu}$. The contributions are logarithmically divergent and only cancel if $g_q = g_l$. To estimate the natural size of such corrections in the model with $g_q = 2g_l$, we imagine that there is some heavy vectorlike fermion with mass m_F and charges such that it cancels the UV contributions of the SM fermions to ϵ at scales above m_F. Then, in the infrared one finds

$$\epsilon \cong \frac{e g_q}{24\pi^2} \ln\left(\frac{m_t^4}{m_b^2 m_\mu m_F}\right) \sim 0.036 g_q e, \qquad (37)$$

where we have taken $m_F = 100$ TeV to get the numerical estimate. This provides an example of how loop effects from the coupling of new physics to leptons (in this case μ) can be important for the coupling to quarks relevant for direct detection, as has been discussed with respect to leptophilic dark matter models in Ref. [70].

Kinetic mixing leads to the effective interaction

$$\frac{\epsilon e g_\chi}{m_{Z'}^2}(\bar{\chi}\gamma^\mu \chi)(\bar{p}\gamma_\mu p) \qquad (38)$$

between DM and protons. The cross section on protons is then

$$\sigma_p = \frac{(\epsilon e g_\chi m_p)^2}{\pi m_{Z'}^4} \sim \frac{1.7 \times 10^{-45}}{\hat{m}_{70}^2}\ \text{cm}^2, \qquad (39)$$

where m_p is the proton mass, and we have used Eqs. (33) and (37). This is just below the current limit of 1.8×10^{-45} cm^2 on protons for 70 GeV DM from the PandaX-II experiment [71], and well above the expected reach of LZ experiment, 1×10^{-47} cm^2 for DM coupling to protons.

B. Light Z', Majorana dark matter

Here we discuss an alternative scenario in which TeV-scale DM annihilates into highly boosted light Z' bosons, whose subsequent decays into b quarks produce antiprotons with a sharply peaked spectrum, to explain a tentative bump at high energies in the AMS-02 data.

[4] We correct an erroneous factor of 4 in their formula.

TABLE II. The values on the left are the best-fit values of dark matter mass and self-annihilation cross section for explaining the $\bar{p}$ excess as determined in Ref. [27]. These fits were done considering mediators of mass 5 GeV which decay to light quarks ($q = u$, d) for the three standard propagation parameter sets. On the right are the values of m_χ that give roughly the same prompt spectrum of $\bar{p}$ when the mediator has a mass of 12 GeV and decays exclusively to b quarks (see Fig. 5). Also listed are necessary cross sections to achieve the same dark matter annihilation rate for these masses.

	$\chi\chi \to q\bar{q}$ $m_{Z'} = 5$ GeV		$\chi\chi \to b\bar{b}$ $m_{Z'} = 12$ GeV	
Propagation model	m_χ [GeV]	$\langle\sigma v\rangle$ [10^{-26}cm^3/s]	m_χ [GeV]	$\langle\sigma v\rangle$ [10^{-26}cm^3/s]
MIN	765	$18.6^{+10.7}_{-8.0}$	1800	103^{+59}_{-44}
MED	808	$5.2^{+3.0}_{-2.4}$	1950	31^{+18}_{-14}
MAX	826	$2.29^{+1.3}_{-1.1}$	1950	$12.8^{+7.3}_{-5.9}$

1. Antiproton spectrum

Reference [27] recently observed that heavy DM, with $m_\chi \sim (0.6\text{–}1)$ TeV, annihilating into light mediators of mass $\sim$5 GeV that decay to u and d quarks, can lead to a spectrum of $\bar{p}$ that fits the AMS-02 excess at high energies. The decay products are highly boosted and result in $\bar{p}$'s that have a spectrum peaked near 300 GeV as observed. The required annihilation cross sections, depending upon different models of cosmic ray propagation, are listed in Table II. These sets of propagation parameters are not the standard ones that appear in the literature (e.g., Ref. [72]), but rather a more recent fit to the proton flux and B/C ratio as measured by AMS-02 [73].

The best-fit values of $\langle\sigma v\rangle$ show that dark matter explanations of the excess tend to require an annihilation cross section above the thermal relic value, 2.3×10^{-26} cm^3/s for 800 GeV DM [54], suggesting that a complete model should have a mechanism, such as Sommerfeld enhancement, for boosting the late-time annihilation cross section relative to that in the early Universe.

The prompt $\bar{p}$ spectrum produced by dark matter annihilation in this scenario is found by boosting the spectrum of $\bar{p}$ from the decays of two Z' bosons at rest. It is given by [27]

$$\frac{dN(x)}{dx} = 2\int_{a(x)}^{b(x)} dx' \frac{1}{\sqrt{1-E_1^2}\sqrt{x'^2 - E_0^2}} \frac{dN(x')}{dx'}, \qquad (40)$$

where $x = E/m_\chi$, E is the total energy, $x' = 2E'/m_{Z'}$, $E_1 = m_{Z'}/m_\chi$, and $E_0 = 2m_{\bar{p}}/m_{Z'}$. The upper and lower limits of integration are $a(x) = x_-$ and $b(x) = \min\{1, x_+\}$ with $x_\pm = 2(x \pm \sqrt{(1-E_1^2)(x^2 - E_1^2 E_0^2/4)})/E_1^2$. Therefore the prompt spectrum of $\bar{p}$ from a dark matter annihilation in this model is determined by m_χ, $m_{Z'}$ and the spectrum of $\bar{p}$ from a single Z' decay. For the latter, we use the tabulated spectra in the PPPC 4 DM ID [74,75].

In Ref. [27], it was assumed that Z' decays with equal strength into light quarks $q = u, d$, whereas in our model, it decays predominantly to b quarks. We find that, to achieve nearly the same shape of the spectrum for $Z' \to b\bar{b}$ as for decays to $q\bar{q}$, we require larger values of both the DM and Z' masses, as shown in Fig. 5. For such a light (12 GeV) Z', fits to $b \to s\mu^+\mu^-$ should be in terms of $g_q g_l/(m_{Z'}^2 - m_b^2)$, leading to a 12% reduction in the required size of $g_q g_l$ compared to the $m_{Z'} \gg m_b$ limit. More importantly, since the rate of annihilation in the Galaxy scales as $n_\chi^2\langle\sigma v\rangle$ and $n_\chi \sim 1/m_\chi$, we need to increase the target values of $\langle\sigma v\rangle$ accordingly. As in the previous section, we consider $g_q \gtrsim 2g_l$ so that decays to leptons can be ignored. The rescaled cross sections and dark matter masses relevant for our model are shown in the right side of Table II.

Fermi-LAT searches for DM annihilation in dwarf spheroidal galaxies currently exclude annihilation cross sections of $\langle\sigma v\rangle > 42 \times 10^{-26}$ cm^3/s at 95% C.L. for 1.95 TeV DM annihilating to $b\bar{b}$ [57], in tension with the value needed to explain the $\bar{p}$ excess with the MIN propagation model. Reference [27] has shown that the tension is ameliorated for the case of interest where $\chi\bar{\chi} \to b\bar{b}b\bar{b}$.

2. Dark matter model

To avoid stringent constraints from direct detection with such a light mediator, we wish to forbid vector couplings of the Z' to χ. A simple model that accomplishes this, while also explaining the origin of the Z' mass, has the Lagrangian [76]

$$\mathcal{L} = \bar{\chi}(i\partial\!\!\!/ - g_\chi Z\!\!\!/' - M)\chi - \left(\frac{f}{\sqrt{2}}\phi\bar{\chi}\chi^c + \text{H.c.}\right) + |(\partial_\mu - 2ig_\chi Z'_\mu)\phi|^2 - \lambda'\left(|\phi|^2 - \frac{1}{2}w^2\right)^2, \qquad (41)$$

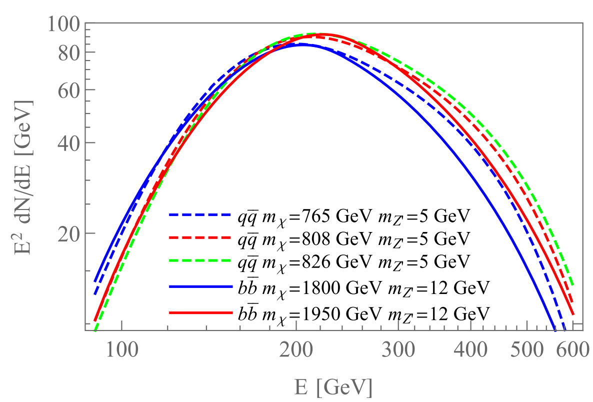

FIG. 5. Antiproton spectra from $\chi\chi \to Z'Z' \to b\bar{b}b\bar{b}$ for $m_{Z'} = 12$ GeV and several dark matter masses, compared to the best fit $\chi\chi \to Z'Z' \to q\bar{q}q\bar{q}$ spectra found in Ref. [27].

where χ is a Dirac particle and the scalar potential causes ϕ to get a VEV $\langle\phi\rangle \equiv w/\sqrt{2}$. After symmetry breaking, χ splits into two Majorana states $\chi_\pm = \frac{1}{\sqrt{2}}(\chi \pm \chi^c)$, with masses $M_\pm = M \pm fw$. The resulting dark sector Lagrangian includes the terms

$$\begin{aligned}\mathcal{L} \ni & \frac{1}{2}\sum_\pm \bar{\chi}_\pm (i\partial\!\!\!/ - M_\pm)\chi_\pm - \frac{g_\chi}{2}(\bar{\chi}_+ Z\!\!\!/' \chi_- + \text{H.c.}) \\ & - \frac{1}{2}\sum_\pm \pm f\varphi\bar{\chi}_\pm\chi_\pm + \frac{1}{2}(\partial_\mu\varphi\partial^\mu\varphi - m_\varphi^2\varphi^2) \\ & + \frac{1}{2}m_{Z'}^2 Z'_\mu Z'^\mu + 2g_\chi^2 Z'_\mu Z'^\mu(2w\varphi + \varphi^2), \end{aligned} \qquad (42)$$

where φ is a dark Higgs boson defined by $\phi = \frac{1}{\sqrt{2}}(w + \varphi)$, $m_\varphi = (2\lambda')^{1/2} w$, and $m_{Z'}^2 = (2g_\chi w)^2 + (g_q\langle\Phi_q\rangle)^2 + (g_l\langle\Phi_l\rangle)^2$.

Recall that the fields $\Phi_{q,l}$ were introduced in Eq. (1) for generating Yukawa couplings that would otherwise be forbidden by the U(1)′ symmetry. In order to help keep $m_{Z'}$ sufficiently light, we assume here that $\langle\Phi_l\rangle \ll \langle\Phi_q\rangle$ so that its contribution to $m_{Z'}$ can be neglected. Moreover we adhere to the relatively small values of $g_q = 2g_l = 0.4 m_{Z'}/\text{TeV} = 0.005$ that were preferred in the heavy Z' scenario, but now in order to keep $g_q\langle\Phi_q\rangle \cong 4.2$ GeV sufficiently small (recalling our assumption that $\langle\Phi_q\rangle \cong M_t \cong 870$ GeV to obtain the observed top Yukawa coupling).

Using these values, $m_{Z'}$ is generated primarily by the first term $2g_\chi w \cong 11$ GeV. We take these parameter values as an example; it would be possible to choose somewhat larger $g_{q,l}$, allowing for the Z' to get somewhat more of its mass from $\langle\Phi_q\rangle$ at the expense of smaller values of w. It will become apparent that taking too small values of w would violate a technical assumption we make below for simplifying the analysis of Sommerfeld enhancement in χ annihilation.

A key feature of this model is that as long as $fw \gtrsim 50$ keV, there are no constraints from direct detection since the ground state χ_- does not have enough energy to produce χ_+ in an inelastic collision with a nucleus. The tree-level decay $\chi_+ \to \chi_-\nu_\mu\bar{\nu}_\mu$ mediated by a Z' is kinematically allowed even for such small mass splittings, so in the present day the dark matter is made up entirely of χ_-.

We note that it would not be natural to make $m_\varphi \gg m_{Z'}$ since both are of order w, so a consistent treatment demands that we include it in the Lagrangian. Doing so also avoids problems with tree-level unitarity that would occur in models with axial couplings of light Z' vector bosons to heavy DM [77]. In the present case, we will find that dark Higgs exchange plays an important role by providing a Sommerfeld enhancement of DM annihilations in the Galactic halo.

3. Relic density

The couplings of $\chi_\pm$ to both Z' and φ after breaking of the $U(1)'$ symmetry lead to several annihilation processes that can affect the DM relic abundance; these include $\chi_\pm\chi_\pm \to Z'Z'$ and $\chi_+\chi_- \to Z'\varphi$. Also present is $\chi_\pm\chi_\pm \to \varphi\varphi$, but it is p-wave suppressed and so we neglect it. Since the $\bar{p}$ signal requires $m_{Z'} \ll m_{\chi_-}$, we expand the cross section in powers of $m_{Z'}/m_{\chi_-}$ and keep only the leading terms. As noted above, the dark Higgs mass cannot be much larger than $m_{Z'}$, so we neglect terms suppressed by $m_\varphi/m_{\chi_\pm}$. In the kinematic threshold approximation $v_{\rm rel} \cong 0$, the annihilation cross sections are

$$\langle\sigma v\rangle_{\chi_\pm\chi_\pm\to Z'Z'} \cong \frac{g_\chi^4}{16\pi m_{\chi_-}^2}\left(1 - 2\frac{f m_{Z'}}{g_\chi m_{\chi_-}}\right), \qquad (43)$$

$$\langle\sigma v\rangle_{\chi_+\chi_-\to Z'\varphi} \cong \frac{(g_\chi^2 - f^2)^2}{16\pi m_{\chi_-}^2}\left(1 - \frac{f m_{Z'}}{g_\chi m_{\chi_-}}\right). \qquad (44)$$

Both $\delta m_\chi = 2fw$ and $m_{Z'} \cong 2g_\chi w$ are proportional to w, so the χ mass splitting must also be $\lesssim 10$ GeV (but not so small that inelastic scattering with nuclei becomes possible). Therefore it is a good approximation to take $m_{\chi_+} \cong m_{\chi_-}$ in estimating the relic density. The effective annihilation cross section in this limit is [78]

$$\begin{aligned}\langle\sigma v\rangle_{\rm eff} = & \frac{1}{4}\langle\sigma v\rangle_{\chi_+\chi_+\to Z'Z'} + \frac{1}{2}\langle\sigma v\rangle_{\chi_+\chi_-\to Z'\varphi} \\ & + \frac{1}{4}\langle\sigma v\rangle_{\chi_-\chi_-\to Z'Z'}. \end{aligned} \qquad (45)$$

The coefficients for $\chi_\pm\chi_\pm \to Z'Z'$ are half that for $\chi_\pm\chi_\mp \to Z'\phi$ because the former process has identical Majorana fermions in the initial state. The correct relic density in this case requires $\langle\sigma v\rangle_{\rm eff} \cong 2.3 \times 10^{-26}$ cm^3/s [54], giving a relationship between g_χ and f,

$$g_\chi^4 + (g_\chi^2 - f^2)^2 \cong \begin{cases} 0.75, & \text{MED, MAX} \\ 0.64, & \text{MIN} \end{cases}, \qquad (46)$$

as shown in Fig. 6.

From Fig. 6 we see that $g_\chi \cong 0.9$ for $f \lesssim 0.8$, and therefore $g_\chi/m_{Z'} \cong 75/\text{TeV}$, in contrast to the couplings of Z' to the SM particles, $(g_q g_l)^{1/2}/m_{Z'} \lesssim 1/\text{TeV}$. This scenario thus requires a substantial hierarchy $g_\chi \gtrsim 75(g_q, g_l)$, which might require additional model-building to seem natural. Here we defer such questions and focus on the phenomenology.

4. Sommerfeld enhancement

At low temperatures $T < \delta m_\chi = m_{\chi_+} - m_{\chi_-}$, long after freeze-out, only the ground state DM χ_- is present: even for very small mass splittings, the tree-level decay channel

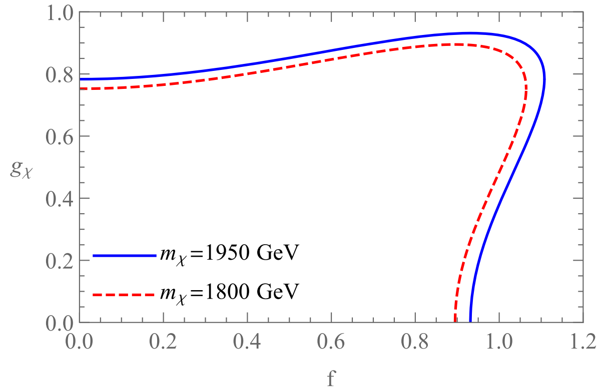

FIG. 6. Values of g_χ and f that give the correct relic density for $m_\chi = 1950$ GeV (MED and MAX propagation models) and $m_\chi = 1800$ GeV (MIN model).

$\chi_+ \to \chi_- \nu_\mu \bar{\nu}_\mu$ by virtual Z' emission is always open. The χ_- annihilation cross section at threshold is given by Eq. (43). For this to be large enough to give a significant $\bar{p}$ signal, we need to be on the horizontal branch of the relic density curves in Fig. 6, where $g_\chi \sim 0.75$–0.9. This range corresponds to a cross section of $(2.3$–$4.0) \times 10^{-26}$ cm^3/s.

To match the central values needed for the AMS signal, we therefore require respective Sommerfeld enhancement factors of order $S \sim 3, 8, 45$ for the MAX, MED, MIN propagation models. To compute the enhancement in the present model accurately could be complicated, because it can generally be mediated both by ϕ and Z' exchange, and the latter interactions are inelastic.

However it turns out that this complication is avoided in our preferred region of parameter space, because the DM mass splitting is so large that Z' exchange is suppressed. Reference [79] shows that the criterion for neglecting Sommerfeld enhancement through Z' exchange is $\delta m_\chi > \alpha'^2 M_\chi/2 = (2.5$–$4)$ GeV, where $\alpha' = g_\chi^2/4\pi$. Since $m_{Z'} = 2 g_\chi w$ and $\delta m_\chi = 2 f w$, this puts a lower bound on the Yukawa coupling, $f \gtrsim 0.14$–0.3, which we will show is satisfied. In contrast, dark Higgs exchange proceeds through diagonal interactions with χ, and since $m_\varphi \ll m_\chi$, it can give rise to Sommerfeld-enhanced annihilation despite the suppression of Z' exchange.

We estimate the enhancement factor from ϕ exchange using [80]

$$S = |\Gamma(a_+)\Gamma(a_-)/\Gamma(1 + 2iu)|^2, \tag{47}$$

where $a_\pm = 1 + iu(1 \pm \sqrt{1 - x/u})$, $x = f^2/(16\pi\beta)$, $\beta = v/c$, $u = 6\beta m_\chi/(\pi^2 m_\varphi)$, for dark matter with velocity v in the center-of-mass frame, which we take to be $v = 10^{-3}c$. The resulting correlated values of m_φ and f needed to fit the antiproton excess are shown in Fig. 7 for the three cosmic ray propagation models. The required values of f are consistent with our assumption of

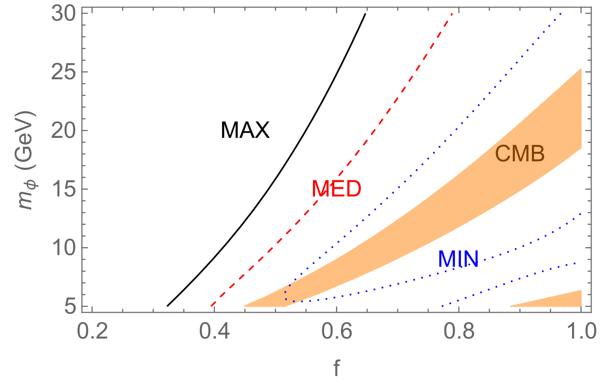

FIG. 7. Values of m_φ versus f that give the observed antiproton excess at high energies, for the respective cosmic ray propagation models as labeled. The orange region is excluded by CMB constraints for DM with $m_\chi = 1800$ GeV. For all curves g_χ is taken to be the value that gives the correct relic density [Eq. (46)]. Where two values of g_χ give the correct relic density (see Fig. 6 where g_χ can be double-valued), the larger one is used, since this requires a smaller Sommerfeld enhancement for the Galactic $\bar{p}$ signal.

sufficiently large DM mass splittings (of order a few GeV) to justify the neglect of Z' exchange in the enhancement factor, and m_φ can be of the same order as $m_{Z'}$ as expected.

Models with significant Sommerfeld enhancement are constrained by their potential to distort the cosmic microwave background (CMB) or disrupt big bang nucleosynthesis (BBN) [81,82]. These effects can be significant since the DM velocity is smaller during BBN and at recombination than at present in the Milky Way halo, possibly leading to a large enhancement of the annihilation cross section at those times. However, the Sommerfeld enhancement saturates at $v_{\rm min} \sim (m_\varphi/m_\chi)c$, which for the values of m_φ and m_χ we consider above is $\sim 10^3$ km/s.

In our scenario, DM kinetically decouples from the Z' bosons when they become nonrelativistic at a temperature of $T \sim m_{Z'}/3$. The most probable velocity of the χ particles is subsequently given by [83]

$$v_0 \approx 10^{-8} \left(\frac{1+z}{600}\right) \sqrt{\left(\frac{\rm MeV}{m_{Z'}}\right)\left(\frac{\rm GeV}{m_\chi}\right)}. \tag{48}$$

For $m_\chi = 1800$ GeV and $m_{Z'} = 12$ GeV, $v_0 \sim 2 \times 10^{-12}$ m/s at $z = 600$, the redshift at which ionization due to DM annihilations can have the strongest effect on the CMB. As this is far below the saturation velocity, changes in DM velocity have little effect on the amount of Sommerfeld enhancement during this epoch, so we assume that S is constant.

With this approximation, we can use the 95% C.L. limits on DM annihilation from the Planck Collaboration [84]

$$S\langle\sigma v\rangle_{\chi\chi\to Z'Z'} f_{\rm eff} < 8.2\times10^{-28}\,\frac{\rm cm^3}{\rm s}\left(\frac{m_\chi}{\rm GeV}\right). \quad (49)$$

We take the efficiency parameter $f_{\rm eff}$ for annihilation to $\bar{b}b$ from Ref. [85]. It has been shown in Ref. [86] that limits from the CMB are insensitive to whether one considers DM annihilating directly to b quarks or to mediators which cascade to b quarks, as occurs in our model. The limits from the CMB when $m_\chi = 1800$ GeV are shown in Fig. 7. In general the amount of Sommerfeld enhancement we need to explain the $\bar{p}$ results is not enough to violate the CMB bounds. Moreover current constraints from BBN are weaker than those from the CMB, with observations of the ratio of deuterium to hydrogen constraining $\langle\sigma v\rangle \lesssim 1100\times10^{-26}$ cm^3/s at 95% C.L. [87] for $m_\chi = 1800$ GeV.

5. Direct detection and collider constraints

We avoid dark matter interactions with protons by Z' exchange (due to kinetic mixing) because of the highly inelastic nature of the coupling $\bar{\chi}_+ Z'\chi_-$. But the dark matter can have a Higgs portal interaction from $\kappa|H|^2|\phi|^2$, allowing the scalar ϕ to mix with the Higgs; the cross section on nucleons is of order

$$\sigma_N \cong \frac{(y_h f\theta m_N)^2}{\pi m_\varphi^4}, \quad (50)$$

where $y_h \cong 10^{-3}$ is the Higgs-nucleon coupling and $\theta\sim\kappa v w/m_h^2$ is the mixing angle (with $v = 246$ GeV). It can be kept below current constraints by taking $f\theta \lesssim 10^{-3}$, assuming that $m_\varphi \sim m_{Z'}$. This implies $\kappa \lesssim 0.025$.

Our model escapes potentially stringent limits from monojets and dijets [88] by its small couplings to quarks, $g_q \lesssim 0.01$. In the dimuon channel, limits on light Z' bosons are significant if $g_q \sim g_l \sim 0.01$ for all flavors of quarks [89,90], but these are relaxed for our model which couples mainly to b quarks. A weak constraint comes from the kinetic mixing coupling and its implications for *BABAR* searches, electroweak precision data [91] and proposed higher-energy collider searches. The natural value of the kinetic mixing parameter is of order $\epsilon \lesssim 5\times10^{-4}$ [see Eq. (37)], which is below the sensitivity of *BABAR* searches for $e^+e^-\to Z'\gamma$, $Z'\to e^+e^-, \mu^+\mu^-$ [92] (and our model is also slightly outside the mass range to which they are sensitive, $m_{Z'} < 10.2$ GeV).

Higher-mass regions can be probed in future collider studies [93], but these also lack the sensitivity to probe such small ϵ. In contrast, the search for Higgs decays $h\to Z'Z'\to 4\ell$ constrains the Higgs portal coupling $\kappa|H|^2|\phi|^2$ to be $\kappa \lesssim 5\times10^{-4}$ [94], though this analysis only applies for $m_{Z'} > 15$ GeV, and would be slightly weakened by the branching ratio for hadronic decay $Z'\to b\bar{b}$ in our model. For such small values of κ the branching ratio for $h\to\varphi\varphi$ is of order $(\kappa v/m_b)^2 \cong 10^{-3}$ and thus does not provide any significant constraint.

V. CONCLUSIONS

The observed anomalies in B-meson decays governed by $b\to s\ell^+\ell^-$ can be explained if there is new physics in $b\to s\mu^+\mu^-$. In this paper we have presented a model with a new Z' vector boson that can explain the anomalies. The model assumes that the SM flavor symmetries are gauged, and that these symmetries are spontaneously broken, leaving only $U(1)'$ at the TeV scale. The Z' is the gauge boson associated with this $U(1)'$, and it couples only to left-handed third-generation quarks and second-generation leptons in the flavor basis. When one transforms to the mass basis, a Z'-mediated $b\to s\mu^+\mu^-$ decay is generated. Taking into account all constraints on the model ($B_s^0-\bar{B}_s^0$ mixing, $b\to s\nu\bar{\nu}$, neutrino trident production), we show that the anomalous decays $B\to K\mu^+\mu^-$ can be explained.

Dark matter annihilation into b quarks is a favored scenario for indirect signals, making it natural to try to link it to anomalies in B-meson decays. We have demonstrated that, by allowing the Z' to also couple to (quasi-)Dirac dark matter χ, one can find a common explanation of the $b\to s\mu^+\mu^-$ anomalies and tentative evidence for excess antiprotons in AMS-02 data. Two alternative scenarios are interesting: a heavy Z' and relatively light χ to explain excess $\bar{p}$'s of energy ~10 GeV, and a light Z' with heavy DM to generate $\bar{p}$'s at ~300 GeV.

Although we did not emphasize it, the heavy-Z'/light-DM scenario has the added advantage of also explaining the persistent gamma-ray excess from the Galactic center observed by Fermi-LAT [95–97]. Thanks to its suppressed couplings to light quarks, our model satisfies stringent limits from direct detection [98,99]. Millisecond pulsars have been suggested as an astrophysical origin for the gamma ray excess, but it remains questionable whether they can plausibly account for all of it [100], leaving the dark matter hypothesis as an interesting possibility.

Both of our proposed scenarios live in regions of parameter space that make them imminently testable by a variety of experimental techniques. The heavy-Z'/light-DM case requires couplings of Z' that put it close to bounds from $B_s-\bar{B}_s$ mixing, and to the sensitivity of LHC searches for $Z'\to\mu^+\mu^-$. In our model, lower than usual Z' masses are allowed by LHC dilepton searches because of the invisible branching ratio from Z' decays to dark matter. At the same time, the natural one-loop level of kinetic mixing of Z' with the photon implies that the DM candidate is just below the current sensitivity of direct detection searches. For the light-Z'/heavy-DM case, a light (~10 GeV) dark Higgs ϕ must also couple to the DM, splitting the Dirac χ into Majorana particles with a large enough mass splitting to be safe from direct detection. The coupling of ϕ to the SM Higgs is already highly constrained by searches for $h\to Z'Z'\to 4\mu$, suggesting that this is the most likely discovery channel at colliders.

ACKNOWLEDGMENTS

We thank Wolfgang Altmannshofer, Kazunori Kohri, Matthew McCullough, Maxim Pospelov, and Sam Witte for helpful discussions or correspondence. We also thank Grace Dupuis for assistance with MADGRAPH. This work was financially supported by NSERC of Canada and by FQRNT of Québec (JMC, JMC).

[1] R. Aaij *et al.* (LHCb Collaboration), Test of Lepton Universality Using $B^+ \to K^+\ell^+\ell^-$ Decays, Phys. Rev. Lett. **113**, 151601 (2014).
[2] R. Aaij *et al.* (LHCb Collaboration), Measurement of Form-Factor-Independent Observables in the Decay $B^0 \to K^{*0}\mu^+\mu^-$, Phys. Rev. Lett. **111**, 191801 (2013).
[3] R. Aaij *et al.* (LHCb Collaboration), Angular analysis of the $B^0 \to K^{*0}\mu^+\mu^-$ decay using 3 fb^{-1} of integrated luminosity, J. High Energy Phys. 02 (2016) 104.
[4] A. Abdesselam *et al.* (Belle Collaboration), Angular analysis of $B^0 \to K^*(892)^0\ell^+\ell^-$, arXiv:1604.04042.
[5] S. Descotes-Genon, T. Hurth, J. Matias, and J. Virto, Optimizing the basis of $B \to K^*ll$ observables in the full kinematic range, J. High Energy Phys. 05 (2013) 137.
[6] S. Descotes-Genon, L. Hofer, J. Matias, and J. Virto, Global analysis of $b \to s\ell\ell$ anomalies, J. High Energy Phys. 06 (2016) 092.
[7] R. Aaij *et al.* (LHCb Collaboration), Differential branching fraction and angular analysis of the decay $B_s^0 \to \phi\mu^+\mu^-$, J. High Energy Phys. 07 (2013) 084.
[8] R. Aaij *et al.* (LHCb Collaboration), Angular analysis and differential branching fraction of the decay $B_s^0 \to \phi\mu^+\mu^-$, J. High Energy Phys. 09 (2015) 179.
[9] R. R. Horgan, Z. Liu, S. Meinel, and M. Wingate, Calculation of $B^0 \to K^{*0}\mu^+\mu^-$ and $B_s^0 \to \phi\mu^+\mu^-$ Observables Using Form Factors from Lattice QCD, Phys. Rev. Lett. **112**, 212003 (2014).
[10] R. R. Horgan, Z. Liu, S. Meinel, and M. Wingate, Rare B decays using lattice QCD form factors, *Proc. Sci.*, LATTICE2014 (2015) 372.
[11] A. Bharucha, D. M. Straub, and R. Zwicky, $B \to V\ell^+\ell^-$ in the standard model from light-cone sum rules, J. High Energy Phys. 08 (2016) 098.
[12] G. Hiller and M. Schmaltz, R_K and future $b \to s\ell\ell$ physics beyond the standard model opportunities, Phys. Rev. D **90**, 054014 (2014).
[13] D. A. Sierra, F. Staub, and A. Vicente, Shedding light on the $b \to s$ anomalies with a dark sector, Phys. Rev. D **92**, 015001 (2015).
[14] G. Bélanger, C. Delaunay, and S. Westhoff, Dark matter relic from muon anomalies, Phys. Rev. D **92**, 055021 (2015).
[15] A. Celis, W. Z. Feng, and M. Vollmann, Dirac dark matter and $b \to s\ell^+\ell^-$ with $\mathbf{U(1)}$ gauge symmetry, Phys. Rev. D **95**, 035018 (2017).
[16] W. Altmannshofer, S. Gori, S. Profumo, and F. S. Queiroz, Explaining dark matter and B decay anomalies with an $L_\mu - L_\tau$ model, J. High Energy Phys. 12 (2016) 106.
[17] M. Aguilar *et al.* (AMS Collaboration), Antiproton Flux, Antiproton-to-Proton Flux Ratio, and Properties of Elementary Particle Fluxes in Primary Cosmic Rays Measured with the Alpha Magnetic Spectrometer on the International Space Station, Phys. Rev. Lett. **117**, 091103 (2016).
[18] B. Grinstein, M. Redi, and G. Villadoro, Low scale flavor gauge symmetries, J. High Energy Phys. 11 (2010) 067.
[19] M. E. Albrecht, T. Feldmann, and T. Mannel, Goldstone bosons in effective theories with spontaneously broken flavour symmetry, J. High Energy Phys. 10 (2010) 089.
[20] R. Alonso, E. F. Martinez, M. B. Gavela, B. Grinstein, L. Merlo, and P. Quilez, Gauged lepton flavour, J. High Energy Phys. 12 (2016) 119.
[21] D. Guadagnoli, R. N. Mohapatra, and I. Sung, Gauged flavor group with left-right symmetry, J. High Energy Phys. 04 (2011) 093.
[22] A. Crivellin, J. Fuentes-Martin, A. Greljo, and G. Isidori, Lepton flavor non-universality in B decays from dynamical yukawas, Phys. Lett. B **766**, 77 (2017).
[23] D. A. Sierra, M. Dhen, C. S. Fong, and A. Vicente, Dynamical flavor origin of $\mathbb{Z}_N$ symmetries, Phys. Rev. D **91**, 096004 (2015).
[24] B. Petersen, M. Ratz, and R. Schieren, Patterns of remnant discrete symmetries, J. High Energy Phys. 08 (2009) 111.
[25] A. Cuoco, M. Krämer, and M. Korsmeier, Novel dark matter constraints from antiprotons in the light of AMS-02, arXiv:1610.03071 [Phys. Rev. Lett. (to be published)].
[26] M. Y. Cui, Q. Yuan, Y. L. S. Tsai, and Y. Z. Fan, A possible dark matter annihilation signal in the AMS-02 antiproton data, arXiv:1610.03840.
[27] X. J. Huang, C. C. Wei, Y. L. Wu, W. H. Zhang, and Y. F. Zhou, Antiprotons from dark matter annihilation through light mediators and a possible excess in AMS-02 $\bar{p}/p$ data, Phys. Rev. D **95**, 063021 (2017).
[28] I. Cholis, D. Hooper, and T. Linden, Evidence for the stochastic acceleration of secondary antiprotons by supernova remnants, arXiv:1701.04406.
[29] R. S. Chivukula and H. Georgi, Composite Technicolor Standard Model, Phys. Lett. B **188**, 99 (1987).
[30] L. J. Hall and L. Randall, Weak scale Effective Supersymmetry, Phys. Rev. Lett. **65**, 2939 (1990).
[31] ATLAS Collaboration, Report No. ATLAS-CONF-2017-015.
[32] L. Calibbi, A. Crivellin, and T. Ota, Effective Field Theory Approach to $b \to s\ell\ell^{(\prime)}$, $B \to K^{(*)}\nu\bar{\nu}$ and $B \to D^{(*)}\tau\nu$ with Third Generation Couplings, Phys. Rev. Lett. **115**, 181801 (2015).

[33] B. Bhattacharya, A. Datta, J. P. Guévin, D. London, and R. Watanabe, Simultaneous explanation of the R_K and $R_{D^{(*)}}$ puzzles: A model analysis, J. High Energy Phys. 01 (2017) 015.

[34] C. Bobeth, M. Gorbahn, T. Hermann, M. Misiak, E. Stamou, and M. Steinhauser, $B_{s,d} \to l^+l^-$ in the Standard Model with Reduced Theoretical Uncertainty, Phys. Rev. Lett. **112**, 101801 (2014).

[35] Y. Amhis *et al.* (Heavy Flavor Averaging Group (HFAG) Collaboration), Averages of b-hadron, c-hadron, and τ-lepton properties as of summer 2014, arXiv:1412.7515.

[36] J. Charles, A. Höcker, H. Lacker, S. Laplace, F. R. Diberder, J. Malclés, J. Ocariz, M. Pivk, and L. Roos, *CP* violation and the CKM matrix: Assessing the impact of the asymmetric B factories, Eur. Phys. J. C **41**, 1 (2005).

[37] A. Hocker, H. Lacker, S. Laplace, and F. Le Diberder, A new approach to a global fit of the CKM matrix, Eur. Phys. J. C **21**, 225 (2001).

[38] J. P. Lees *et al.* (*BABAR* Collaboration), Search for $B \to K^{(*)}\nu\bar{\nu}$ and invisible quarkonium decays, Phys. Rev. D **87**, 112005 (2013).

[39] O. Lutz *et al.* (Belle Collaboration), Search for $B \to h^{(*)}\nu\bar{\nu}$ with the full Belle $\Upsilon(4S)$ data sample, Phys. Rev. D **87**, 111103 (2013).

[40] A. J. Buras, J. Girrbach-Noe, C. Niehoff, and D. M. Straub, $B \to K^{(*)}\nu\bar{\nu}$ decays in the standard model and beyond, J. High Energy Phys. 02 (2015) 184.

[41] K. Koike, M. Konuma, K. Kurata, and K. Sugano, Neutrino production of lepton pairs. 1. -, Prog. Theor. Phys. **46**, 1150 (1971).

[42] K. Koike, M. Konuma, K. Kurata, and K. Sugano, Neutrino production of lepton pairs. 2.-, Prog. Theor. Phys. **46**, 1799 (1971).

[43] R. Belusevic and J. Smith, W—Z interference in neutrino—nucleus scattering, Phys. Rev. D **37**, 2419 (1988).

[44] R. W. Brown, R. H. Hobbs, J. Smith, and N. Stanko, Intermediate boson. iii. virtual-boson effects in neutrino trident production, Phys. Rev. D **6**, 3273 (1972).

[45] W. Altmannshofer, S. Gori, M. Pospelov, and I. Yavin, Neutrino Trident Production: A Powerful Probe of New Physics with Neutrino Beams, Phys. Rev. Lett. **113**, 091801 (2014).

[46] S. R. Mishra *et al.* (CCFR Collaboration), Neutrino Tridents and W Z Interference, Phys. Rev. Lett. **66**, 3117 (1991).

[47] C. Patrignani *et al.* (Particle Data Group Collaboration), Review of particle physics, Chin. Phys. C **40**, 100001 (2016).

[48] J. Alwall, M. Herquet, F. Maltoni, O. Mattelaer, and T. Stelzer, MadGraph 5: Going Beyond, J. High Energy Phys. 06 (2011) 128.

[49] J. Alwall, R. Frederix, S. Frixione, V. Hirschi, F. Maltoni, O. Mattelaer, H. S. Shao, T. Stelzer, P. Torrielli, and M. Zaro, The automated computation of tree-level and next-to-leading order differential cross sections, and their matching to parton shower simulations, J. High Energy Phys. 07 (2014) 079.

[50] W. Altmannshofer, S. Gori, M. Pospelov, and I. Yavin, Quark flavor transitions in $L_\mu - L_\tau$ models, Phys. Rev. D **89**, 095033 (2014).

[51] B. Allanach, F. S. Queiroz, A. Strumia, and S. Sun, Z' models for the LHCb and $g-2$ muon anomalies, Phys. Rev. D **93**, 055045 (2016).

[52] W. Altmannshofer, C. Y. Chen, P. S. B. Dev, and A. Soni, Lepton flavor violating Z' explanation of the muon anomalous magnetic moment, Phys. Lett. B **762**, 389 (2016).

[53] S. Aoki *et al.*, Review of lattice results concerning low-energy particle physics, Eur. Phys. J. C **77**, 112 (2017).

[54] G. Steigman, B. Dasgupta, and J. F. Beacom, Precise Relic WIMP abundance and its impact on searches for dark matter annihilation, Phys. Rev. D **86**, 023506 (2012).

[55] S. J. Lin, X. J. Bi, J. Feng, P. F. Yin, and Z. H. Yu, A systematic study on the cosmic ray antiproton flux, arXiv:1612.04001.

[56] H. Davoudiasl and W. J. Marciano, Running of the U(1) coupling in the dark sector, Phys. Rev. D **92**, 035008 (2015).

[57] M. Ackermann *et al.* (Fermi-LAT Collaboration), Searching for Dark Matter Annihilation from Milky Way Dwarf Spheroidal Galaxies with Six Years of Fermi Large Area Telescope Data, Phys. Rev. Lett. **115**, 231301 (2015).

[58] V. Bonnivard *et al.*, Dark matter annihilation and decay in dwarf spheroidal galaxies: The classical and ultrafaint dSphs, Mon. Not. R. Astron. Soc. **453**, 849 (2015).

[59] P. Ullio and M. Valli, A critical reassessment of particle dark matter limits from dwarf satellites, J. Cosmol. Astropart. Phys. 07 (2016) 025.

[60] ATLAS Collaboration, Report No. ATLAS-CONF-2016-045.

[61] CMS Collaboration, Report No. CMS-PAS-EXO-16-031.

[62] J. M. Cline, G. Dupuis, Z. Liu, and W. Xue, The windows for kinetically mixed Z'-mediated dark matter and the galactic center gamma ray excess, J. High Energy Phys. 08 (2014) 131.

[63] D. A. Faroughy, A. Greljo, and J. F. Kamenik, Confronting lepton flavor universality violation in B decays with high-p_T tau lepton searches at LHC, Phys. Lett. B **764**, 126 (2017).

[64] A. M. Sirunyan *et al.* (CMS Collaboration), Search for dijet resonances in proton–proton collisions at $\sqrt{s} =$ 13 TeV and constraints on dark matter and other models, Phys. Lett. B (to be published), DOI: 10.1016/j.physletb.2017.02.012.

[65] M. Aaboud *et al.* (ATLAS Collaboration), Search for resonances in the mass distribution of jet pairs with one or two jets identified as b-jets in proton–proton collisions at $\sqrt{s} = 13$ TeV with the ATLAS detector, Phys. Lett. B **759**, 229 (2016).

[66] ATLAS Collaboration, Report No. ATLAS-CONF-2016-060.

[67] CMS Collaboration, Report No. CMS-PAS-B2G-15-002.

[68] G. Arcadi, Y. Mambrini, M. H. G. Tytgat, and B. Zaldivar, Invisible Z' and dark matter: LHC vs LUX constraints, J. High Energy Phys. 03 (2014) 134.

[69] D. S. Akerib *et al.* (LZ Collaboration), LUX-ZEPLIN (LZ) conceptual design report, arXiv:1509.02910.

[70] F. D'Eramo, B. J. Kavanagh, and P. Panci, Probing leptophilic dark sectors with hadronic processes, arXiv:1702.00016.

[71] Y. Yang (PandaX-II Collaboration), Search for dark matter from the first data of the PandaX-II experiment, *Proc. Sci.*, ICHEP2016 (2016) 224.

[72] F. Donato, N. Fornengo, D. Maurin, and P. Salati, Antiprotons in cosmic rays from neutralino annihilation, Phys. Rev. D **69**, 063501 (2004).

[73] H. B. Jin, Y. L. Wu, and Y. F. Zhou, Cosmic ray propagation and dark matter in light of the latest AMS-02 data, J. Cosmol. Astropart. Phys. 09 (2015) 049.

[74] M. Cirelli, G. Corcella, A. Hektor, G. Hütsi, M. Kadastik, P. Panci, M. Raidal, F. Sala, and A. Strumia, PPPC 4 DM ID: A poor particle physicist cookbook for dark matter indirect detection, J. Cosmol. Astropart. Phys. 03 (2011) 051.

[75] P. Ciafaloni, D. Comelli, A. Riotto, F. Sala, A. Strumia, and A. Urbano, Weak corrections are relevant for dark matter indirect detection, J. Cosmol. Astropart. Phys. 03 (2011) 019.

[76] D. Tucker-Smith and N. Weiner, Inelastic dark matter, Phys. Rev. D **64**, 043502 (2001).

[77] F. Kahlhoefer, K. Schmidt-Hoberg, T. Schwetz, and S. Vogl, Implications of unitarity and gauge invariance for simplified dark matter models, J. High Energy Phys. 02 (2016) 016.

[78] K. Griest and D. Seckel, Three exceptions in the calculation of relic abundances, Phys. Rev. D **43**, 3191 (1991).

[79] T. R. Slatyer, The Sommerfeld enhancement for dark matter with an excited state, J. Cosmol. Astropart. Phys. 02 (2010) 028.

[80] S. Cassel, Sommerfeld factor for arbitrary partial wave processes, J. Phys. G **37**, 105009 (2010).

[81] J. Hisano, M. Kawasaki, K. Kohri, T. Moroi, K. Nakayama, and T. Sekiguchi, Cosmological constraints on dark matter models with velocity-dependent annihilation cross section, Phys. Rev. D **83**, 123511 (2011).

[82] T. Bringmann, F. Kahlhoefer, K. Schmidt-Hoberg, and P. Walia, Strong Constraints on Self-Interacting Dark Matter with Light Mediators, Phys. Rev. Lett. **118**, 141802 (2017).

[83] M. Cirelli, P. Panci, K. Petraki, F. Sala, and M. Taoso, Dark Matter's secret liaisons: phenomenology of a dark U(1) sector with bound states, arXiv:1612.07295.

[84] P. A. R. Ade *et al.* (Planck Collaboration), Planck 2015 results. XIII. Cosmological parameters, Astron. Astrophys. **594**, A13 (2016).

[85] T. R. Slatyer, Indirect dark matter signatures in the cosmic dark ages. I. Generalizing the bound on s-wave dark matter annihilation from Planck results, Phys. Rev. D **93**, 023527 (2016).

[86] G. Elor, N. L. Rodd, T. R. Slatyer, and W. Xue, Model-independent indirect detection constraints on hidden sector dark matter, J. Cosmol. Astropart. Phys. 06 (2016) 024.

[87] M. Kawasaki, K. Kohri, T. Moroi, and Y. Takaesu, Revisiting big-bang nucleosynthesis constraints on dark-matter annihilation, Phys. Lett. B **751**, 246 (2015).

[88] M. Chala, F. Kahlhoefer, M. McCullough, G. Nardini, and K. Schmidt-Hoberg, Constraining dark sectors with monojets and dijets, J. High Energy Phys. 07 (2015) 089.

[89] I. Hoenig, G. Samach, and D. Tucker-Smith, Searching for dilepton resonances below the Z mass at the LHC, Phys. Rev. D **90**, 075016 (2014).

[90] A. Alves, G. Arcadi, Y. Mambrini, and F. S. Queiroz, Augury of darkness: The low-mass dark Z' portal, arXiv:1612.07282.

[91] A. Hook, E. Izaguirre, and J. G. Wacker, Model independent bounds on kinetic mixing, Adv. High Energy Phys. **2011**, 859762 (2011).

[92] J. P. Lees *et al.* (*BABAR* Collaboration), Search for a dark photon in e^+e^- collisions at BABAR, Phys. Rev. Lett. **113**, 201801 (2014).

[93] D. Curtin, R. Essig, S. Gori, and J. Shelton, Illuminating dark photons with high-energy colliders, J. High Energy Phys. 02 (2015) 157.

[94] E. Castaneda-Miranda, Z-dark search with the ATLAS detector, J. Phys. Conf. Ser. **761**, 012081 (2016).

[95] T. Daylan, D. P. Finkbeiner, D. Hooper, T. Linden, S. K. N. Portillo, N. L. Rodd, and T. R. Slatyer, The characterization of the gamma-ray signal from the central Milky Way: A case for annihilating dark matter, Phys. Dark Univ. **12**, 1 (2016).

[96] F. Calore, I. Cholis, and C. Weniger, Background model systematics for the Fermi GeV excess, J. Cosmol. Astropart. Phys. 03 (2015) 038.

[97] M. Ajello *et al.* (Fermi-LAT Collaboration), Fermi-LAT observations of high-energy γ-ray emission toward the Galactic center, Astrophys. J. **819**, 44 (2016).

[98] D. Hooper, Z' mediated dark matter models for the Galactic center gamma-ray excess, Phys. Rev. D **91**, 035025 (2015).

[99] M. Escudero, D. Hooper, and S. J. Witte, Updated collider and direct detection constraints on dark matter models for the Galactic center gamma-ray excess, J. Cosmol. Astropart. Phys. 02 (2017) 038.

[100] D. Haggard, C. Heinke, D. Hooper, and T. Linden, Low mass x-ray binaries in the inner galaxy: Implications for millisecond pulsars and the GeV excess, arXiv:1701.02726.